Cell Genomics, Volume *2*

Supplemental information

Type 1 diabetes risk genes mediate pancreatic beta cell survival in response to proinflammatory cytokines

Paola Benaglio, Han Zhu, Mei-Lin Okino, Jian Yan, Ruth Elgamal, Naoki Nariai, Elisha Beebe, Katha Korgaonkar, Yunjiang Qiu, Margaret K.R. Donovan, Joshua Chiou, Gaowei Wang, Jacklyn Newsome, Jaspreet Kaur, Michael Miller, Sebastian Preissl, Sierra Corban, Anthony Aylward, Jussi Taipale, Bing Ren, Kelly A. Frazer, Maike Sander, and Kyle J. Gaulton

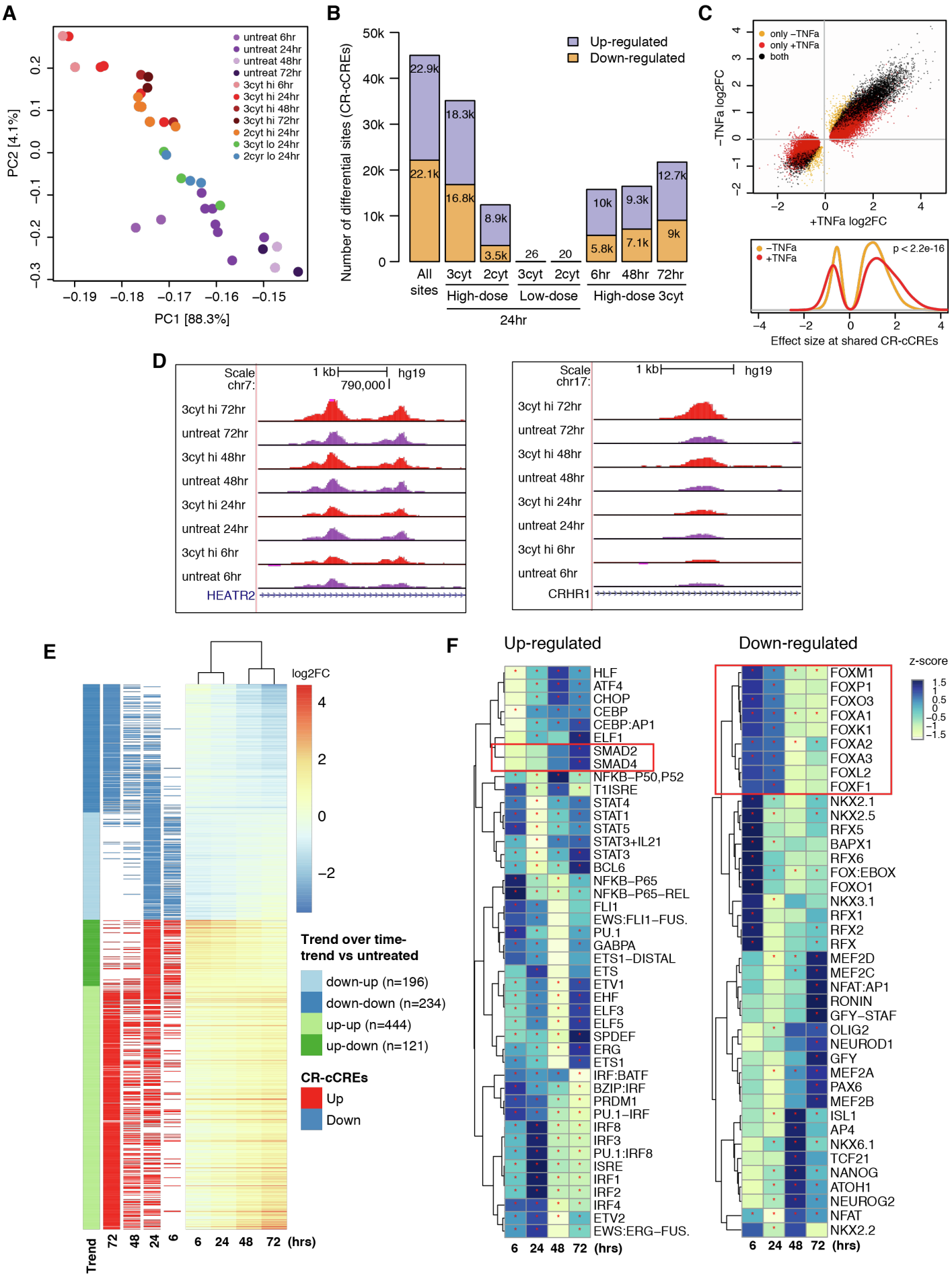
A
untreat 6hr
untreat 24hr
untreat 48hr
untreat 72hr
3cyt hi 6hr
3cyt hi 24hr
3cyt hi 48hr
3cyt hi 72hr
2cyt hi 24hr
3cyt lo 24hr
2cyr lo 24hr
PC2 [4.1%]
PC1 [88.3%]
B
Up-regulated
Down-regulated
Number of differential sites (CR-cCREs)
All sites
3cyt
2cyt
High-dose
Low-dose
High-dose 3cyt
24hr
C
only −TNFa
only +TNFa
both
−TNFa log2FC
+TNFa log2FC
p < 2.2e-16
Effect size at shared CR-cCREs
D
Scale
chr7:
1 kb
790,000
hg19
HEATR2
chr17:
CRHR1
E
log2FC
Trend over time-trend vs untreated
down-up (n=196)
down-down (n=234)
up-up (n=444)
up-down (n=121)
CR-cCREs
Up
Down
Trend
(hrs)
F
Up-regulated
Down-regulated
z-score
HLF
ATF4
CHOP
CEBP
CEBP:AP1
ELF1
SMAD2
SMAD4
NFKB−P50,P52
T1ISRE
STAT4
STAT1
STAT5
STAT3+IL21
STAT3
BCL6
NFKB−P65
NFKB−P65−REL
FLI1
EWS:FLI1−FUS.
PU.1
GABPA
ETS1−DISTAL
ETS
ETV1
EHF
ELF3
ELF5
SPDEF
ERG
ETS1
IRF:BATF
BZIP:IRF
PRDM1
PU.1−IRF
IRF8
IRF3
PU.1:IRF8
ISRE
IRF1
IRF2
IRF4
ETV2
EWS:ERG−FUS.
FOXM1
FOXP1
FOXO3
FOXA1
FOXK1
FOXA2
FOXA3
FOXL2
FOXF1
NKX2.1
NKX2.5
RFX5
BAPX1
RFX6
FOX:EBOX
FOXO1
NKX3.1
RFX1
RFX2
RFX
MEF2D
MEF2C
NFAT:AP1
RONIN
GFY−STAF
OLIG2
NEUROD1
GFY
MEF2A
PAX6
MEF2B
ISL1
AP4
NKX6.1
TCF21
NANOG
ATOH1
NEUROG2
NFAT
NKX2.2

Figure S1. Effect of different cytokine treatments on islet accessible chromatin, related to Figure 2. A) Principal component analysis showing distribution of samples (n=35) based on the different cytokine treatments, color-coded as shown in the legend. Hi: high dose; Lo: low dose; 3cyt: IL-1β, IFN-γ, TNFa; 2cyt: IL-1β, IFN-γ. **B**) Number of cytokine-responsive cCREs (CR-cCREs) for each treatment compared to control, and union of all differential sites. **C**) Top: Scatterplot showing effect on cytokine-responsive cCREs (DESeq FDR <0.10) chromatin accessibility in islets after treatment with high doses of three cytokines (IL-1β, IFNγ, and TNFα , x-axis) versus two cytokines (IL-1β and IFNγ, y-axis). Bottom: density plot showing increased effect size in cytokine treatment with TNFα. Wilcoxon signed rank test p-value is shown. **D**) Heatmap of cytokine effect sizes (log_2 fold change, DESeq) on cytokine-responsive cCREs that change with treatment duration (linear regression p< 0.01). **E**) Example of two cytokine-responsive cCREs at the *HEATR2* and *CRHR1* loci that show increased accessibility over time. **F**) Motif enrichment for up-regulated or down-regulated cytokine–responsive cCREs identified using different duration of cytokine treatments. Motifs that were significantly enriched in at least one condition (HOMER FDR<0.05, indicated by an asterisk) are shown. Red boxes highlight motifs with visible differences in enrichment over time.

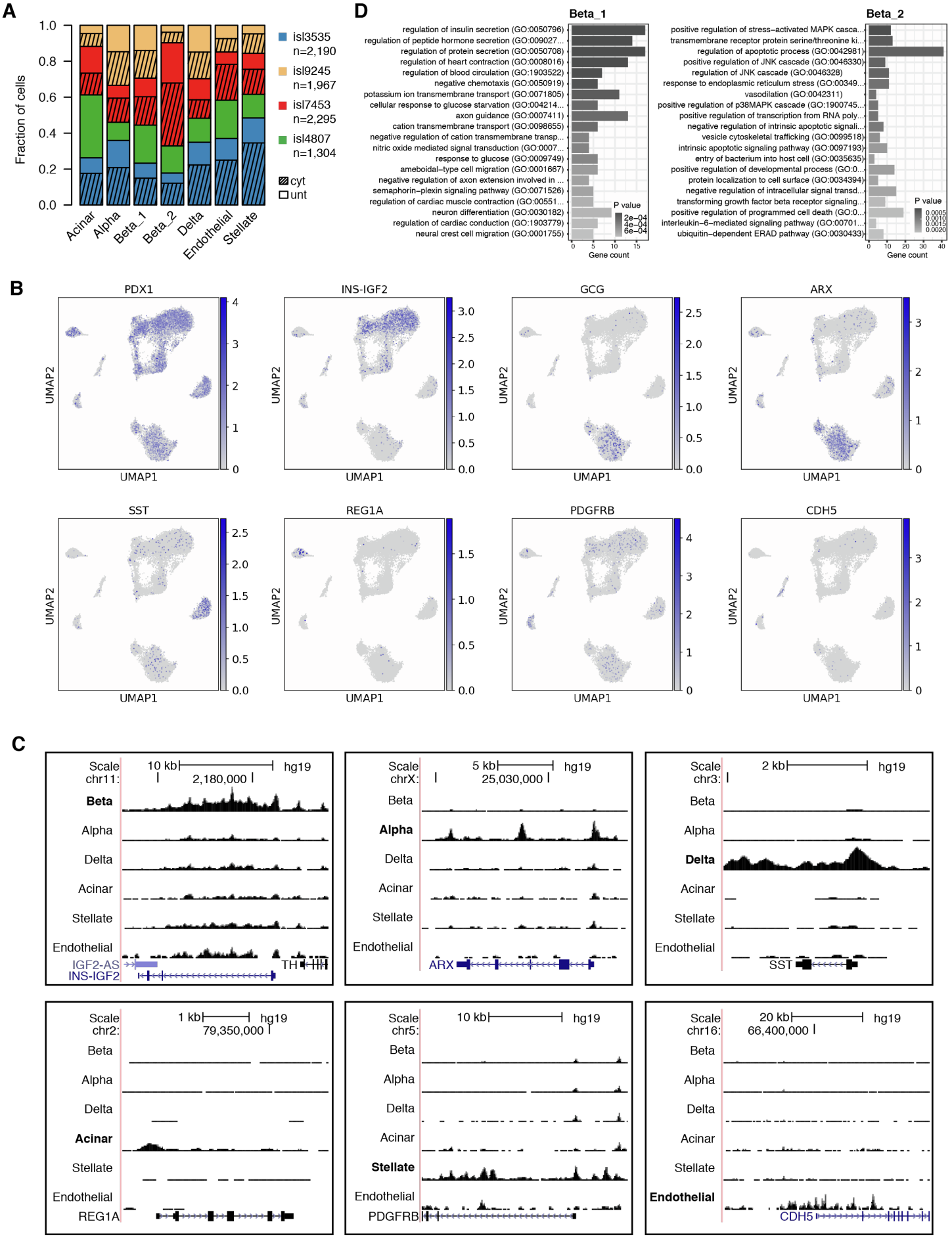
A
Fraction of cells
1.0
0.8
0.6
0.4
0.2
0.0
Acinar
Alpha
Beta_1
Beta_2
Delta
Endothelial
Stellate
isl3535
n=2,190
isl9245
n=1,967
isl7453
n=2,295
isl4807
n=1,304
cyt
unt
D
Beta_1
regulation of insulin secretion (GO:0050796)
regulation of peptide hormone secretion (GO:009027...
regulation of protein secretion (GO:0050708)
regulation of heart contraction (GO:0008016)
regulation of blood circulation (GO:1903522)
negative chemotaxis (GO:0050919)
potassium ion transmembrane transport (GO:0071805)
cellular response to glucose starvation (GO:004214...
axon guidance (GO:0007411)
cation transmembrane transport (GO:0098655)
negative regulation of cation transmembrane transp...
nitric oxide mediated signal transduction (GO:0007...
response to glucose (GO:0009749)
ameboidal−type cell migration (GO:0001667)
negative regulation of axon extension involved in ...
semaphorin−plexin signaling pathway (GO:0071526)
regulation of cardiac muscle contraction (GO:00551...
neuron differentiation (GO:0030182)
regulation of cardiac conduction (GO:1903779)
neural crest cell migration (GO:0001755)
P value
2e−04
4e−04
6e−04
Gene count
Beta_2
positive regulation of stress−activated MAPK casca...
transmembrane receptor protein serine/threonine ki...
regulation of apoptotic process (GO:0042981)
positive regulation of JNK cascade (GO:0046330)
regulation of JNK cascade (GO:0046328)
response to endoplasmic reticulum stress (GO:00349...
vasodilation (GO:0042311)
positive regulation of p38MAPK cascade (GO:1900745...
positive regulation of transcription from RNA poly...
negative regulation of intrinsic apoptotic signali...
vesicle cytoskeletal trafficking (GO:0099518)
intrinsic apoptotic signaling pathway (GO:0097193)
entry of bacterium into host cell (GO:0035635)
positive regulation of developmental process (GO:0...
protein localization to cell surface (GO:0034394)
negative regulation of intracellular signal transd...
transforming growth factor beta receptor signaling...
positive regulation of programmed cell death (GO:0...
interleukin−6−mediated signaling pathway (GO:00701...
ubiquitin−dependent ERAD pathway (GO:0030433)
P value
0.0005
0.0010
0.0015
0.0020
Gene count
B
PDX1
INS-IGF2
GCG
ARX
SST
REG1A
PDGFRB
CDH5
UMAP1
UMAP2
C
Scale
chr11:
10 kb
2,180,000
hg19
Beta
Alpha
Delta
Acinar
Stellate
Endothelial
IGF2-AS
INS-IGF2
TH
Scale
chrX:
5 kb
25,030,000
hg19
ARX
Scale
chr3:
2 kb
SST
Scale
chr2:
1 kb
79,350,000
REG1A
Scale
chr5:
10 kb
PDGFRB
Scale
chr16:
20 kb
66,400,000
CDH5

Figure S2. Defining islet cell sub-types from snATAC-seq profiles, related to Figure 2. **A**) Proportion of cells derived from different donors and treatment conditions in each cluster. **B**) UMAP plots showing promoter accessibility in a 1 kb window around the TSS for selected cell type marker genes. **C**) Genome browser plots showing aggregate read density (CPM-normalized read depth, range: 0-7, shown on vertical axis for each plot) for cells within each cell type for selected cell type marker genes. **D**) Gene Ontology enrichment analysis (Biological_Process_2021 database) for the closest genes to upregulated peaks (logFC >0.5 and FDR<0.05) in Beta_1 and Beta_2 sub-populations.

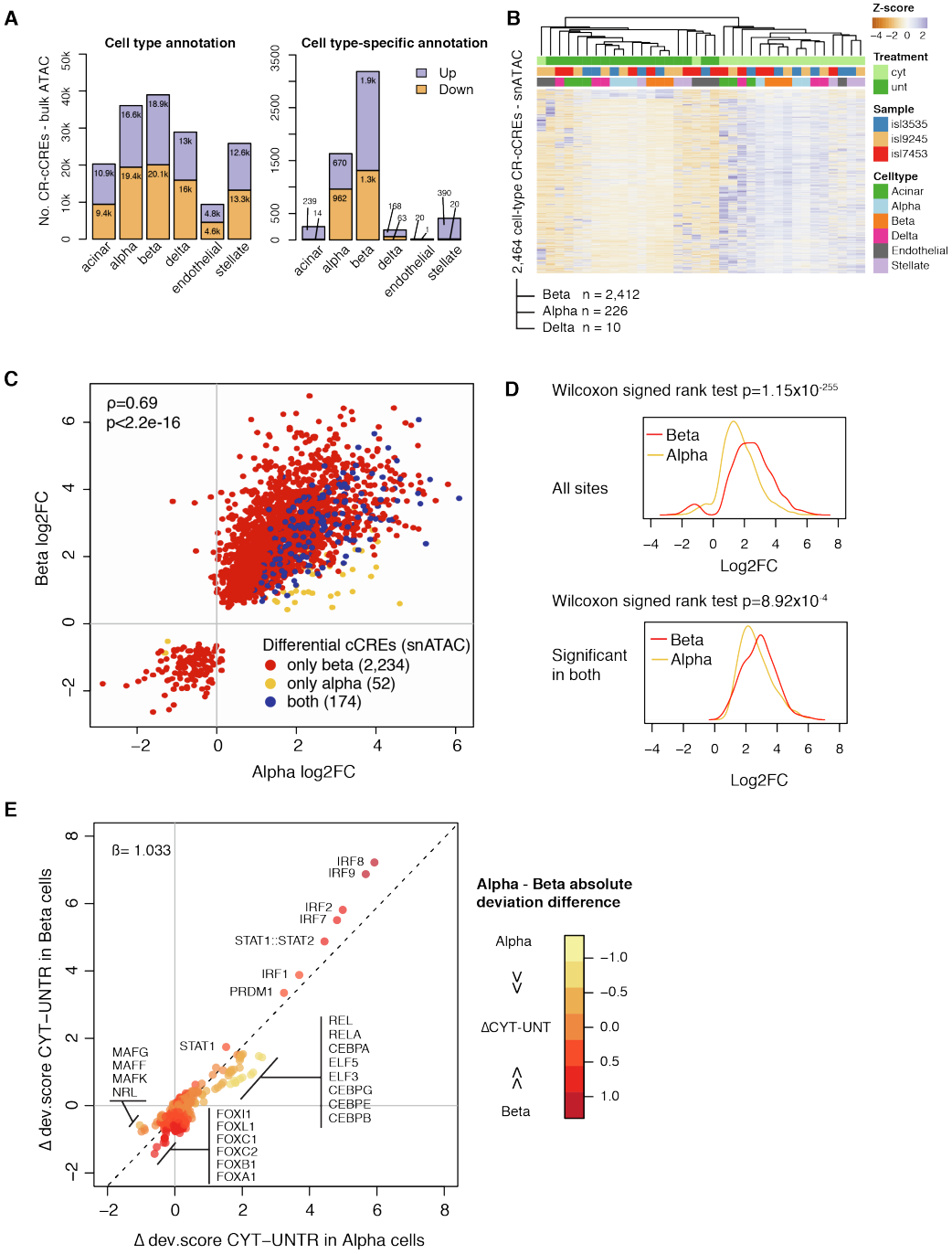

Figure S3. Cell type-specific changes in islet accessible chromatin upon inflammatory cytokine exposure, related to Figure 2. A) Left: Number of cytokine-responsive cCREs in bulk islet ATAC that overlap a snATAC from different cell types. Right: Number of cytokine-responsive cCREs in bulk islet ATAC that overlap a snATAC specific to a cell type. **B**) Heatmap of z-score normalized chromatin accessibility at significant cytokine-responsive cCREs (DESeq FDR<0.1) identified in beta, alpha and delta cells by snATAC comparing cytokine-treated and untreated samples. Endothelial, acinar, and stellate cells did not show any significant cytokine-responsive cCREs. **C**) Scatterplot showing cytokine-responsive cCRE effect sizes (DESeq $\log_2$ fold change) in alpha and beta cells. **D**) Density plot showing increased cytokine response in beta cells at cytokine-responsive cCREs significant in either beta or alpha cells (top), and in cytokine-responsive cCREs significant in both cell types (bottom). **E**) Comparison of motif enrichment in chromatin accessibility from cytokine treated alpha and beta cells. ChromVAR deviation scores within alpha or beta cells were averaged across treated and untreated cells and their difference (ΔCTY-UNT) was plotted in a scatterplot. The slope (ß) from linear regression and the most different motifs between alpha and beta are shown are shown.

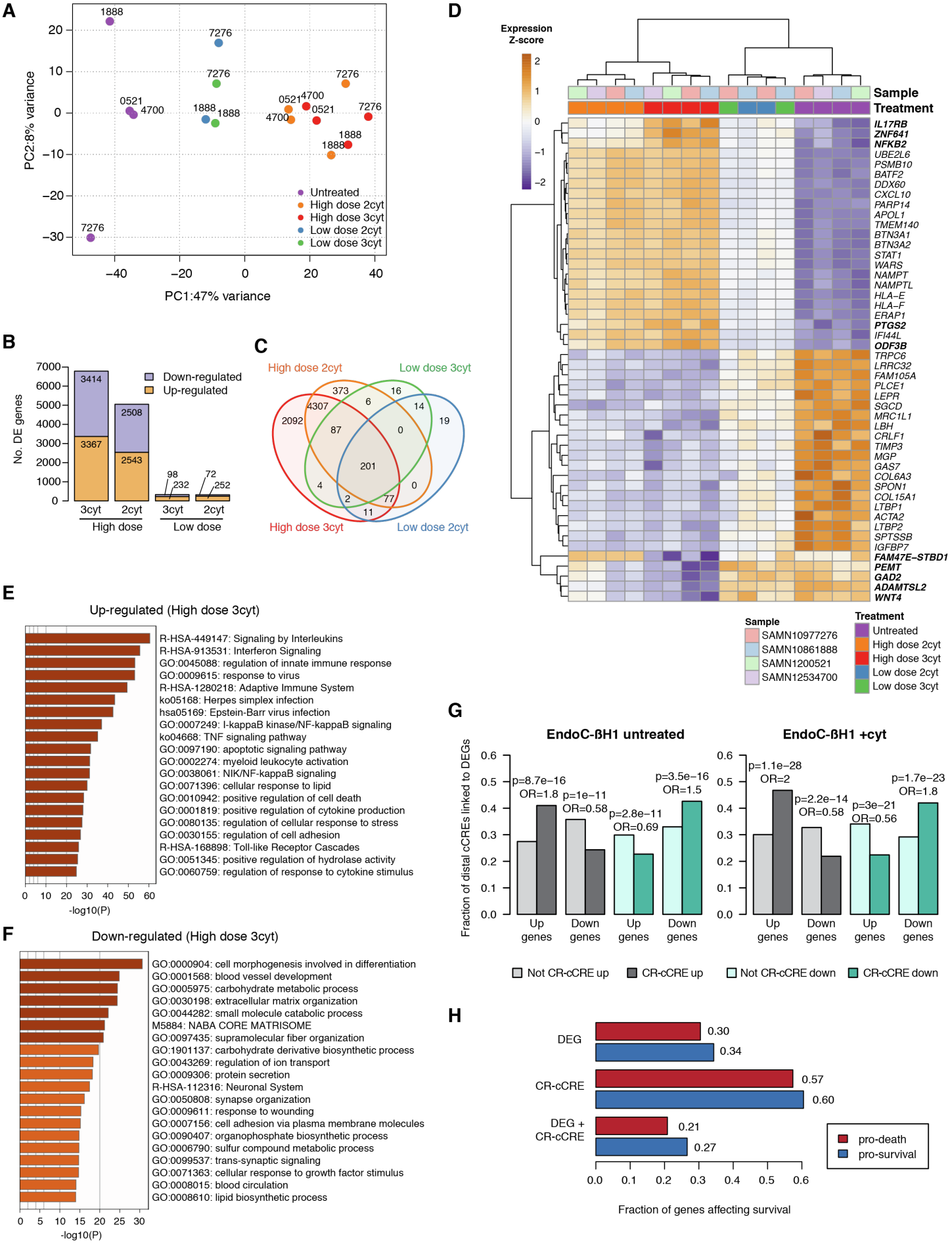
A
PC2:8% variance
PC1:47% variance
Untreated
High dose 2cyt
High dose 3cyt
Low dose 2cyt
Low dose 3cyt
B
No. DE genes
Down-regulated
Up-regulated
3cyt
2cyt
High dose
Low dose
C
High dose 2cyt
Low dose 3cyt
High dose 3cyt
Low dose 2cyt
D
Expression Z-score
Sample
Treatment
IL17RB
ZNF641
NFKB2
UBE2L6
PSMB10
BATF2
DDX60
CXCL10
PARP14
APOL1
TMEM140
BTN3A1
BTN3A2
STAT1
WARS
NAMPT
NAMPTL
HLA–E
HLA–F
ERAP1
PTGS2
IFI44L
ODF3B
TRPC6
LRRC32
FAM105A
PLCE1
LEPR
SGCD
MRC1L1
LBH
CRLF1
TIMP3
MGP
GAS7
COL6A3
SPON1
COL15A1
LTBP1
ACTA2
LTBP2
SPTSSB
IGFBP7
FAM47E–STBD1
PEMT
GAD2
ADAMTSL2
WNT4
SAMN10977276
SAMN10861888
SAMN1200521
SAMN12534700
Untreated
High dose 2cyt
High dose 3cyt
Low dose 2cyt
Low dose 3cyt
E
Up-regulated (High dose 3cyt)
R-HSA-449147: Signaling by Interleukins
R-HSA-913531: Interferon Signaling
GO:0045088: regulation of innate immune response
GO:0009615: response to virus
R-HSA-1280218: Adaptive Immune System
ko05168: Herpes simplex infection
hsa05169: Epstein-Barr virus infection
GO:0007249: I-kappaB kinase/NF-kappaB signaling
ko04668: TNF signaling pathway
GO:0097190: apoptotic signaling pathway
GO:0002274: myeloid leukocyte activation
GO:0038061: NIK/NF-kappaB signaling
GO:0071396: cellular response to lipid
GO:0010942: positive regulation of cell death
GO:0001819: positive regulation of cytokine production
GO:0080135: regulation of cellular response to stress
GO:0030155: regulation of cell adhesion
R-HSA-168898: Toll-like Receptor Cascades
GO:0051345: positive regulation of hydrolase activity
GO:0060759: regulation of response to cytokine stimulus
-log10(P)
F
Down-regulated (High dose 3cyt)
GO:0000904: cell morphogenesis involved in differentiation
GO:0001568: blood vessel development
GO:0005975: carbohydrate metabolic process
GO:0030198: extracellular matrix organization
GO:0044282: small molecule catabolic process
M5884: NABA CORE MATRISOME
GO:0097435: supramolecular fiber organization
GO:1901137: carbohydrate derivative biosynthetic process
GO:0043269: regulation of ion transport
GO:0009306: protein secretion
R-HSA-112316: Neuronal System
GO:0050808: synapse organization
GO:0009611: response to wounding
GO:0007156: cell adhesion via plasma membrane molecules
GO:0090407: organophosphate biosynthetic process
GO:0006790: sulfur compound metabolic process
GO:0099537: trans-synaptic signaling
GO:0071363: cellular response to growth factor stimulus
GO:0008015: blood circulation
GO:0008610: lipid biosynthetic process
-log10(P)
G
EndoC-βH1 untreated
EndoC-βH1 +cyt
Fraction of distal cCREs linked to DEGs
p=8.7e−16 OR=1.8
p=1e−11 OR=0.58
p=2.8e−11 OR=0.69
p=3.5e−16 OR=1.5
p=1.1e−28 OR=2
p=2.2e−14 OR=0.58
p=3e−21 OR=0.56
p=1.7e−23 OR=1.8
Up genes
Down genes
Not CR-cCRE up
CR-cCRE up
Not CR-cCRE down
CR-cCRE down
H
DEG
CR-cCRE
DEG + CR-cCRE
pro-death
pro-survival
Fraction of genes affecting survival

Figure S4. Cytokine-induced gene expression changes in pancreatic islets, related to Figure 3. **A**) Principal components plot of normalized and batch-corrected gene expression from high-dose-2-cytokine (orange), high-dose three cytokine (red) low-dose two cytokine (blue), low-dose three cytokine (green) -treated and untreated (purple) islets from a total of 16 samples. Donor ID is indicated on the top of each dot. **B**) Number of differentially expressed genes (DE genes, DESeq FDR<0.1) between each cytokine treatment condition and untreated islets. **C**) Venn diagram showing overlap between DE genes in each treatment. **D**) Heatmap showing the top 20 upregulated and top 20 downregulated genes common to each treatment vs untreated islets, and the top 10 differential genes (in bold) between high-dose two cytokine and high-dose three cytokine (i.e due to TNFα). **E**) Gene ontology terms enriched among genes with up-regulated expression in cytokine-treated islets. **F**) Gene ontology terms enriched among genes with down-regulated expression in cytokine-treated islets. **G**) Enrichment of islet distal cytokine-responsive cCREs (>10kb from TSS) for genes with concordant cytokine-induced effects, linked by HiChIP (FDR <0.1). Fisher's exact test p-values and odds ratios are shown. HiChIP was performed in untreated (left) or cytokine-treated (right) EndoC-βH1 cells. **H**) Fraction of pro-survival and pro-death genes from the CRISPR screen with differential expression in islets after high-dose cytokine treatment, linked to an islet cytokine-responsive cCRE (CR-cCRE) via co-accessibility, or both.

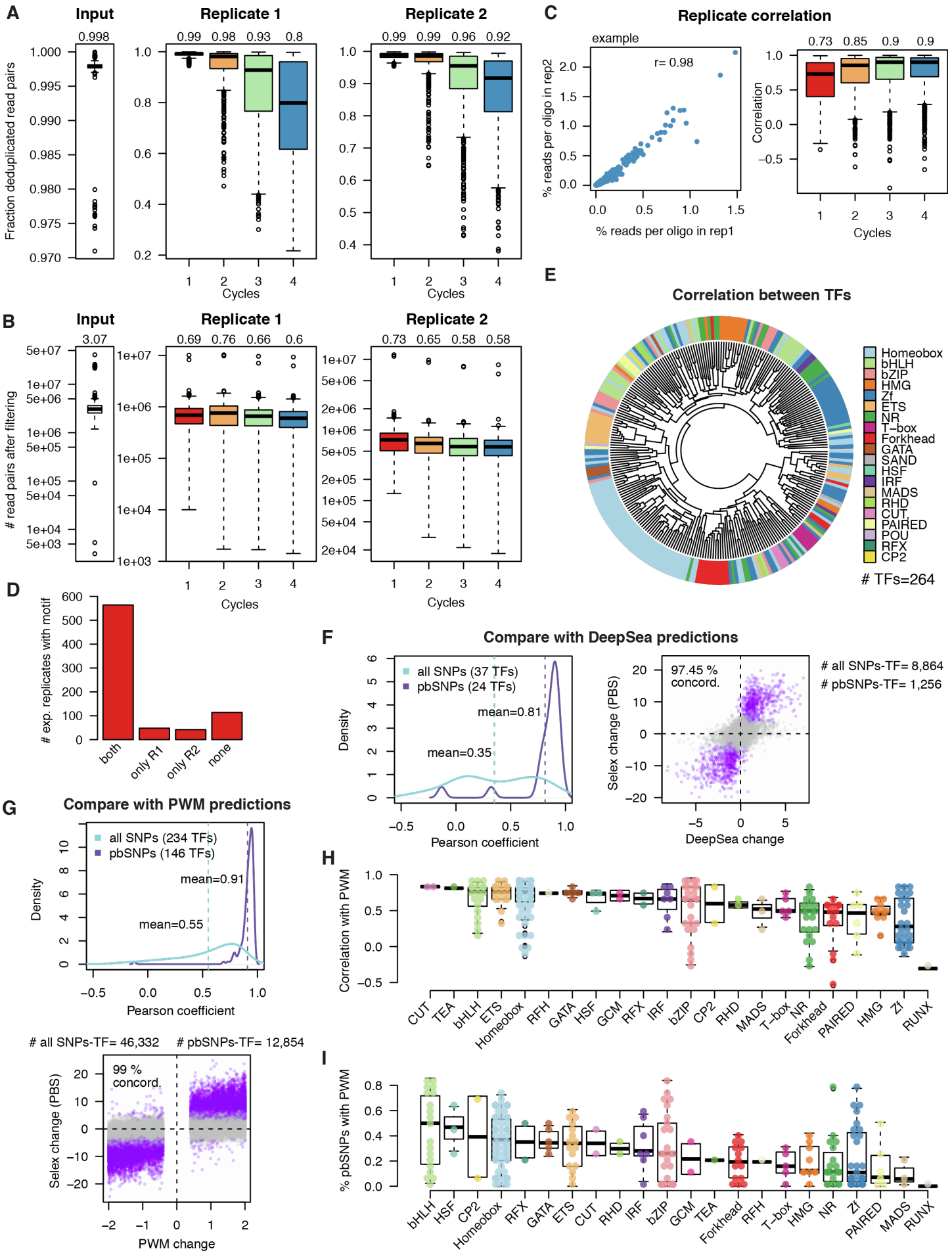
A
Input
Replicate 1
Replicate 2
Fraction deduplicated read pairs
Cycles
B
read pairs after filtering
C
Replicate correlation
example
r= 0.98
% reads per oligo in rep2
% reads per oligo in rep1
Correlation
D
exp. replicates with motif
both
only R1
only R2
none
E
Correlation between TFs
Homeobox
bHLH
bZIP
HMG
Zf
ETS
NR
T−box
Forkhead
GATA
SAND
HSF
IRF
MADS
RHD
CUT
PAIRED
POU
RFX
CP2
TFs=264
F
Compare with DeepSea predictions
all SNPs (37 TFs)
pbSNPs (24 TFs)
mean=0.81
mean=0.35
Density
Pearson coefficient
97.45 %
concord.
Selex change (PBS)
DeepSea change
all SNPs-TF= 8,864
pbSNPs-TF= 1,256
G
Compare with PWM predictions
all SNPs (234 TFs)
pbSNPs (146 TFs)
mean=0.91
mean=0.55
# all SNPs-TF= 46,332
# pbSNPs-TF= 12,854
99 %
concord.
PWM change
H
Correlation with PWM
CUT
TEA
bHLH
ETS
Homeobox
RFH
GATA
HSF
GCM
RFX
IRF
bZIP
CP2
RHD
MADS
T−box
NR
Forkhead
PAIRED
HMG
Zf
RUNX
I
% pbSNPs with PWM
bHLH
HSF
CP2
Homeobox
RFX
GATA
ETS
CUT
RHD
IRF
bZIP
GCM
TEA
Forkhead
RFH
T−box
HMG
NR
Zf
PAIRED
MADS
RUNX

Figure S5. SNP-SELEX sequencing metrics, replicate consistency, and comparison with TF binding predictions, related to Figure 5. **A**) Fraction of reads retained after removing identical sequencing duplicate reads. The input is composed of 384 pools of oligos with different barcodes (from 4x 96-well plates); each SELEX cycle is composed of 768 assays (8x 96-well plates), performed twice. Median value is indicated at the top of each boxplot. **B**) Number of reads retained after removing identical sequencing duplicate reads. The y-axis is log scaled. **C**) Left: example of one experiment showing correlation between the percentages of reads mapping to each oligo (i.e. each dot) in replicate 1 versus replicate 2. Pearson correlation coefficient is indicated. Right: distributions of Pearson coefficients calculated as in the example, across all 768 experiments and cycles. **D**) Number of experiments showing enrichment at cycle 4 for motifs similar to the assayed TF protein in both replicates, only one of the two, and none. **E**) Hierarchical clustering of the pairwise distance (1-correlation) of allelic effects (PBS score) across different TF proteins, color-coded according to the structural family. 264 TFs that had a minimum of 100 testable SNPs are shown. **F**) Left: distribution of correlation between PBS and DeepSea Log fold change across TFs. The number of TFs analyzed (having both DeepSea predictions and SNP-SELEX results for at least 10 SNPs) are indicated. Rigth: scatterplot of PBS and DeepSea Log fold change across tested SNP-TF pairs (number indicated). Preferentially bound SNPs (pbSNPs) are shown in purple. **G**) Top: distribution of correlation between PBS and ΔPWM across TFs. The number of TFs analyzed (having measurements for both PWMs and SNP-SELEX for at least 10 SNPs) are indicated. Bottom: scatterplot of PBS and ΔPWM across all tested SNP-TF pairs (number indicated). pbSNPs are shown in purple. **H**) Pearson correlation coefficients between SNP-SELEX PBS score and ΔPWM in each TF across all bound SNPs, grouped by structural families. 234 TFs that had a minimum of 10 testable SNPs with PWM predicted effects are shown. **I**) Percentage of pbSNPs that corresponded to a predicted PWM change in each TF, grouped by TF family. 234 TFs that had a minimum of 10 testable SNPs with PWM predicted effects are shown

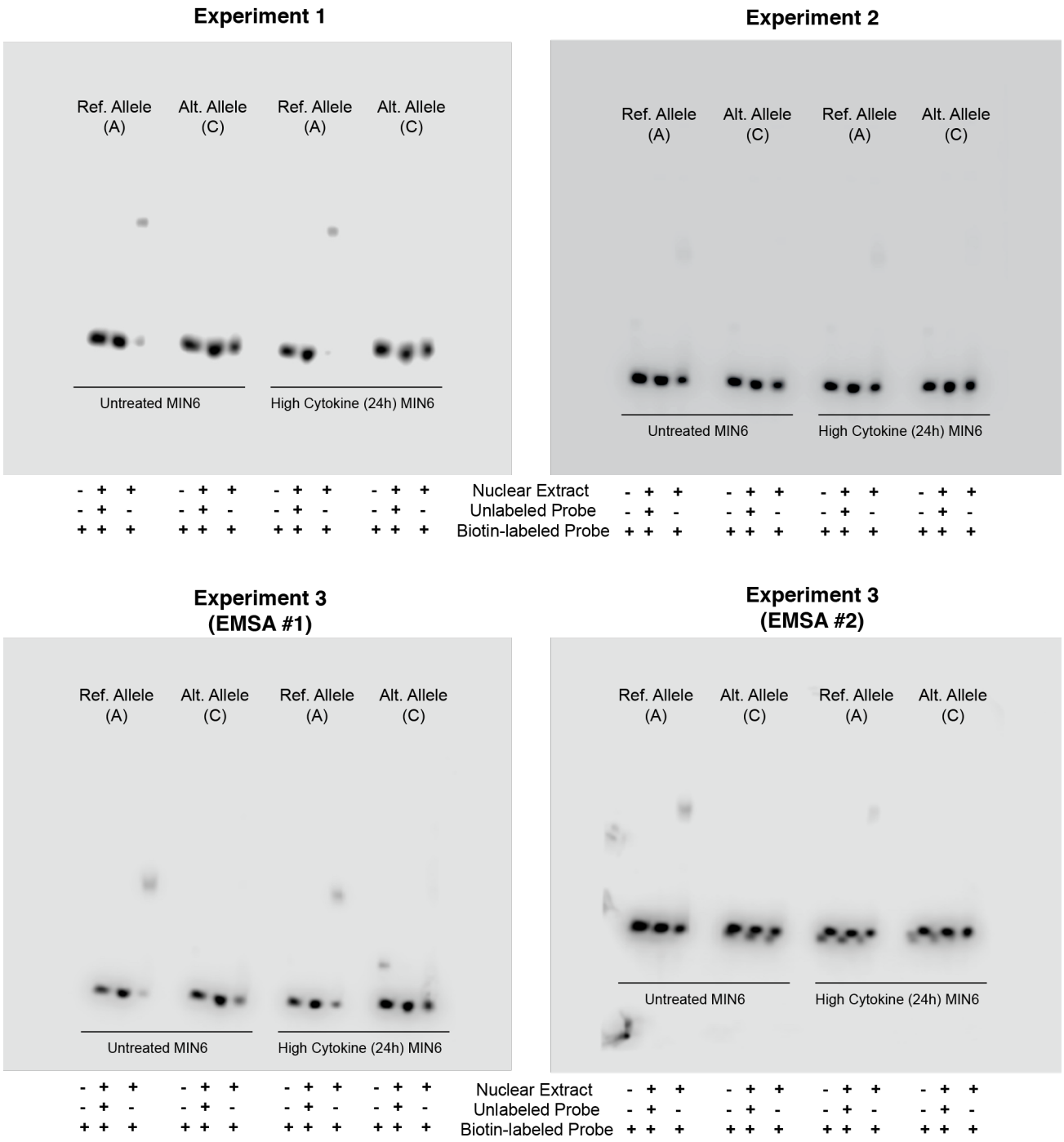

Figure S6. Electrophoretic mobility shift assay (EMSA) for rs35342456 at the *DEXI/SOCS1* locus, related to Figure 6. Three independent EMSA experiments (different cell cultures) and one replicate of binding reaction for experiment #3 are shown. MIN6 were cultured in control and cytokine media and nuclear extracts were used in binding reaction with oligonucleotides carrying either the reference (A) or alternate (C) allele of rs35342456. Both treated and untreated MIN6 cells nuclear extracts showed preferential binding to probes with the reference allele. The top-left panel (Experiment 1) shows the non-cropped image shown in **Figure 6E**.

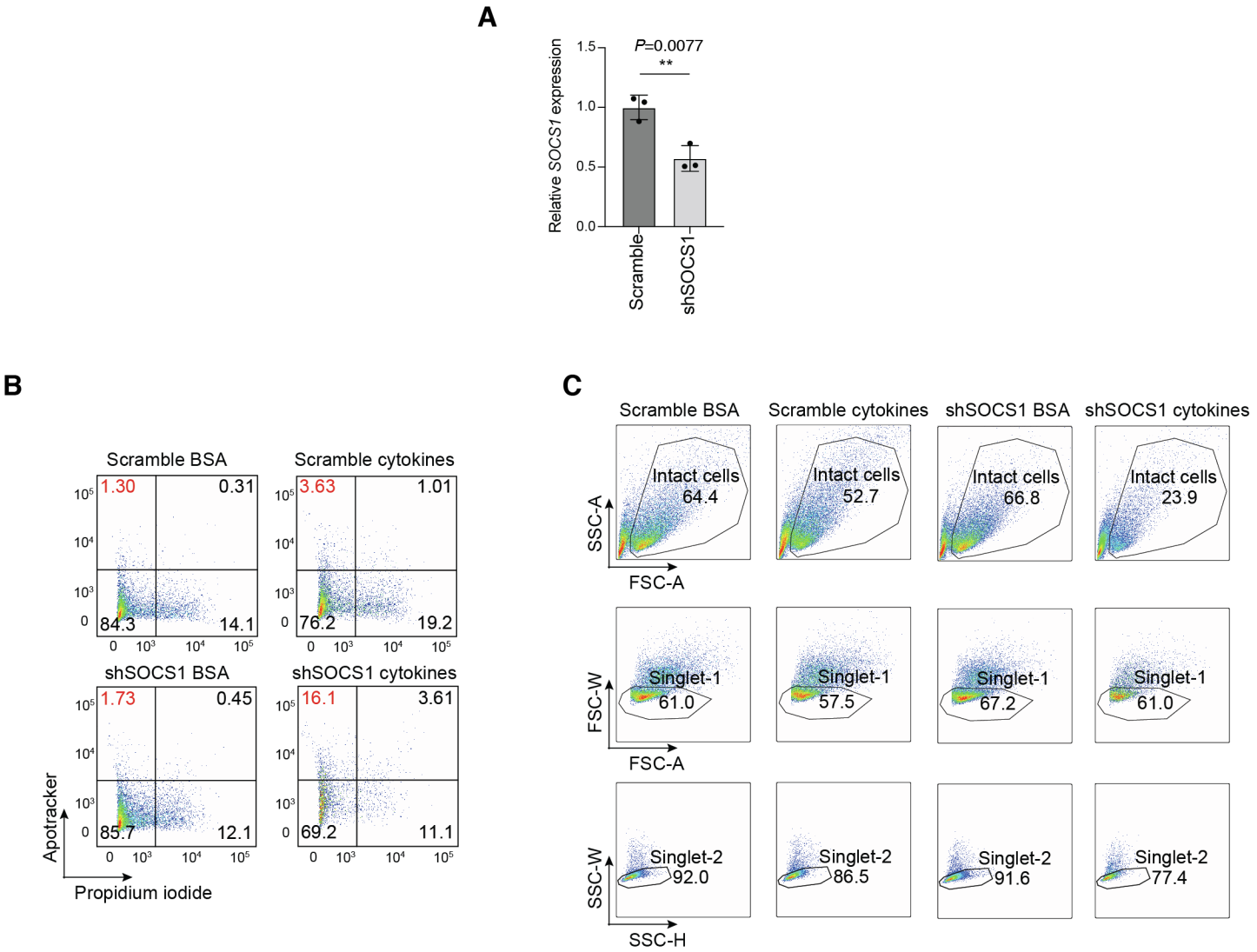

Figure S7. SOCS1 knock-down effect in EndoC-βH1 cells, related to Figure 6. A) qPCR analysis of SOCS1 expression in EndoC-βH1 cells transduced with lentivirus expressing scramble (left) or small hairpin RNA (shRNA) targeting SOCS1. Data was shown as mean ± SD (n=3). P-values were calculated by unpaired two-tailed t-test. **B**) Representative flow cytometry plots showing apoptotic EndoC-βH1 cell (Apotracker+/ Propidium iodide-, highlighted in red) ratio in response to cytokine and vehicle (0.1% BSA) treatment. Apoptotic cells transduced with lentivirus expressing either scramble (left) or small hairpin RNA (shRNA) targeting SOCS1 (right) were compared. **C**) Examples of flow cytometry plots showing gating strategies to obtain plots shown in B.